Iron Oxide Nanostructures Mediated by *Fagonia Indica* Plant Extract: A Green Approach for the Removal of Toxic Organic Dyes Effluent from Waste Water

Saba Naz*, S. Sasui, A. Rizwan, K. Dileep and A. Saba
Dr. M.A. Kazi Institute of Chemistry University of Sindh, Jamshoro.
saba.naz@usindh.edu.pk*

(received on 9th March 2026, accepted in revised form 21st April 2026)

Abstract: Organic dyes are major cause of water pollution and a great threat to living organisms, animals and humans. In this study the iron oxide nanostructures (IONS) were synthesized by using *Fagonia indica* medicinal plant extract for photocatalytic degradation of harmful dyes. Among various synthesis methods, green synthesis is preferred because of its ecological benefits and cost effectiveness. Several techniques like UV-Visible, FTIR, SEM, XRD and DLS were used for characterization of IONS. The maximum absorption of IONS was observed at 294nm by UV –Visible spectroscopy. FTIR revealed significant peaks especially at 845 and 548cm^{-1} corresponding to Fe─O stretching vibration which supports the formation of IONS catalyst. SEM micrographs confirm the angular and agglomerated nature of IONS which was further supported by amorphous pattern observed in XRD analysis. DLS and zeta potential also supported the agglomerated structure showing a particle size of 78.8 nm and a zeta potential of −16mV. Despite agglomeration, it still showed excellent catalytic efficacy because of surface hydroxyl groups and plant mediated functional groups that supress the electron hole recombination and increase reactive oxygen. The IONS showed greater catalytic activity under sunlight approximately 87.5% methylene blue (MB) was degraded within 40 mins with a rate constant of 0.0519min^{-1}.

Graphical Abstract:

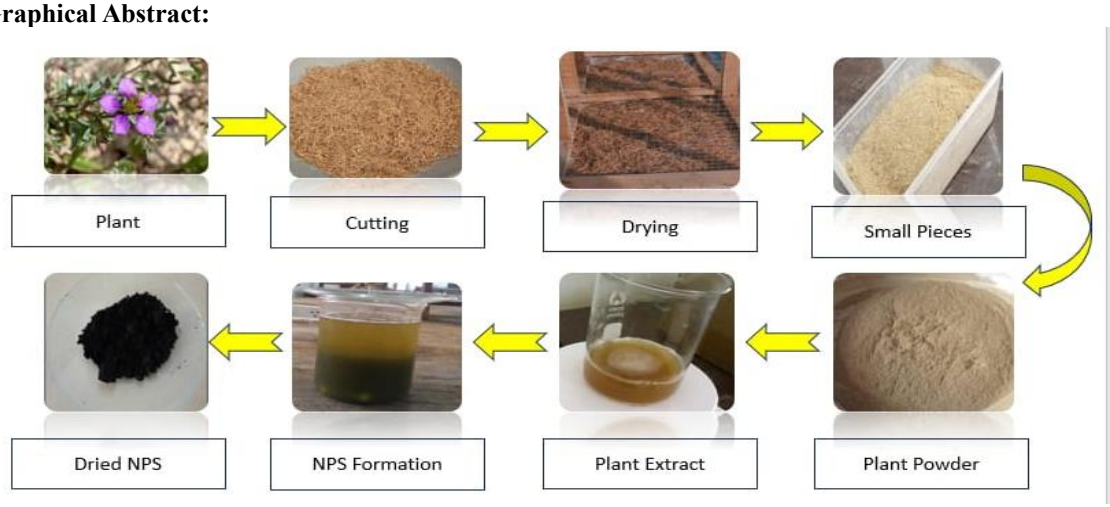

Key words: Fagonia indica, Iron Oxide nanostructures, organic dyes pollutant, photocatalytic degradation

Introduction

Fast industrialization and urbanization cause to the continuous release of dangerous contaminants into natural water systems, presenting severe risk to ecological durability and human health [1-2]. Including these pollutants, fabricated organic dyes discharge from chemical, leather, paper, pharmaceutical and textile industries are of special interest cause of their high stability, complex aromatic structures and resistance to bio-degradation [3-4]. Conventional methods for removing the environmental pollutants are often inefficient motivating the demand for renewable methods [5-7]. Nanotechnology, specifically photocatalysis employing metal oxide nanostructures, provides a sustainable solution for degrading persistent organic pollutants [8-10]. IONS like (FeO, Fe_2O_3, and Fe_3O_4) are favourable photocatalysts due to their activity in visible-light, non-toxicity, chemical stability, and magnetic recoverability The IONS offer great significant advantages over other common photocatalysts like ZnO and TiO_2, which faces the challenges of recovery after

*To whom all correspondence should be addressed.

water treatment [11-13]. Although the efficiency of IONS relay on fabrication methods, size of particles, and surface chemistry [14-16]. Eco-friendly synthesis employing plants, offers a renewable way to synthesized metal oxide NS with phytochemical-mediating surface functionalization and reduction [17-18]. IONS efficiently degrade dyes like methylene blue (MB) in the presence visible light by producing active oxygen species that degrade the dye [19]. In recent years, environmentally benign synthesis have gained considerable attention as sustainable alternatives for conventional nanoparticles/ nanostructures fabrication techniques which rely on biological entities, including plant material, algae, fungi, bacteria and naturally occurring biomolecules, which function as both reducing and capping agents. Plant extracts contain diverse range of bioactive compounds such as flavonoids, phenolic compounds, tannins, terpenoids and saponins that simultaneously drive metal ion reduction and enhance the stability of the synthesized nanomaterials [20]. *Fagonia Indica* (Family Zygophyllaceae) is a widely distributed medicinal plant found across south Asia and Africa. It has been traditionally used in locally prepared herbal medicine due to its diverse therapeutic properties, including antioxidant, anti-inflammatory, antimicrobial, antipyretic, antidiabetic and anticancer activities [21]. Earlier studies have revealed that *Fagonia. Indica* and the other related species can be used for bioreduction and stabilization of metal nanoparticles. Such as Qureshi, K. A., et al, [22]. demonstrated the use of *Fagonia Indica* leaf extract for silver nanoparticles fabrication which exhibited enhanced antioxidant and antimicrobial activities. However, in another study Hussain et al [23] reported the synthesis of metal nanoparticles using *Fagonia Cretica* species for biomedical applications. These studies highlight the contribution and important role of medicinal plants in Nano chemistry and biomedical application. Plant mediated ecofriendly synthesis is usually considered a sustainable approach where green chemicals such as phytochemical acts as reducing and stabilizing agents. Plant extract provides a versatile, cost effective and environmentally benevolent way for nanomaterial synthesis. The main advantage of using plant extract is to eliminate the toxic chemicals with improved biocompatibility and enhanced biological activity [24]. Despite their promising capabilities, the application of *Fagonia indica* mediated iron oxide nanostructures for the degradation of commonly used organic dyes has not been sufficiently investigated in the literature. Therefore, in this study, *Fagonia Indica* plant extract mediated IONS were synthesized through an environmentally friendly method. The synthesized NS were evaluated as a photocatalyst for the degradation of MB under sunlight irradiation and dark conditions to see the visible difference of synthesized NS activity. Comprehensive characterization was carried out to investigate the structural, morphological, and optical properties of the NS, as well as their photocatalytic performance. This work aims to contribute to the development of low cost, sustainable, and eco-friendly nanomaterial for waste water treatment and environmental remediation.

Experimental

Chemicals

All chemicals used in this study were of analytical grade. Ferrous sulphate heptahydrate ($FeSO_4 \cdot 7H_2O$) was purchased from Sigma-Aldrich. Sodium hydroxide (NaOH) pellets were obtained from Merck Millipore. Methylene blue was purchased from Merck, Germany. Deionized water used throughout the experiments was procured from Al-Beruni Scientific Store, Hyderabad, Sindh.

Preparation of Extract

Fagonia Indica was purchased from locally available Shah Medicinal and Herbal store, Hyderabad, Sindh, Pakistan. Plant was thoroughly washed with deionized water to remove any dirt after that it was shade dried and ground into a fine powder. The powder was kept in an oven at 40°C for two hours. In this method 3g of finely grind powdered of *Fagonia Indica* were added in 100 ml of deionized water and kept for heating with continuous stirring in hot plate at 40°C for 2 hours. Then the extract was set aside for overnight and after filtration it was stored at 4°C for further use.

Synthesis of Iron Oxide NS

A total 0.695g of $FeSO_4.7H_2O$ was dissolved in 10 ml of deionized water. Then, 90 ml of the prepared extract was added to the solution. The pH was adjusted to 12, resulting in a rapid colour change that indicated the formation of Ferrous hydroxide $Fe(OH)_2$ precipitate. Because $Fe(OH)_2$ is unstable in oxygen atmosphere it was gradually converted into Ferric hydroxide $Fe(OH)_3$. The mixture was then heated in an oven at 78 °C for 2 hrs to promote the growth of $Fe(OH)_3$ structures. After that the resulting sample was then filtered and calcined at 450°C in a muffle furnace to remove moisture content and conversion to iron oxide nanostructures [25].

Characterization

The synthesized IONS were characterized using various techniques. Uv-Visible spectroscopy confirmed the formation of IONS, showing characteristic absorption in the range of 200-700 nm. Functional groups involved in the synthesis were identified using Fourier

transform infrared (FT-IR) spectroscopy, with spectra recorded from 4000 to 400cm^{-1}. Scanning Electron Microscopy (SEM) was employed to examine the morphology, surface features, and distribution of the NS. The structural properties of the synthesized NS were analysed using X-ray diffraction (XRD). Dynamic light scattering (DLS) provided information on particle size and size distribution in suspension, while zeta potential measurements were performed to evaluate the surface charge and colloidal stability of the NS in an aqueous solution.

Photocatalytic Degradation of Methylene Blue Dye

The photocatalytic degradation of MB was systematically studied to assess the effect of key operational parameters, including solution pH, initial dye concentration, and the dosage of IONS. The effect of solution acidity or alkalinity was examined by measuring degradation efficiency across a range of pH values, while the role initial MB concentration was assessed to understand mass transfer limitations and catalyst surface saturation effects. Additionally, the varying impact of IONS dosage on photocatalytic performance was studied to identify the optimal catalyst loading. After individual assessment of each parameter the three factors were collectively optimized to monitor the effect on MB degradation versus irradiation time until maximum degradation efficiency reached. The MB degradation was analysed under dark conditions and direct sun light, both in presence and absence of IONS. The degradation efficiency was then calculated using the standard relation represented by eq:1 [63].

$$\textbf{Degradation efficiency (\%)} = \frac{C_0 - C_t}{C_0} X\ 100 \quad \textbf{(eq:1)}$$

where C_o represents the initial dye concentration and C_t represents concentration at time t, as determined from UV-Visible measurements. This methodology is widely employed in photocatalytic studies to quantitatively assess dye removal efficiency and to confirm the photocatalytic nature of degradation process rather than the simple adsorption or direct photolysis [27].

Results and Discussion

UV-Vis Spectroscopic Analysis

The Uv−Visible spectroscopy was used to make sure the synthesis and stability of IONS fabricated by *Fagonia Indica* extract. The absorbance were analysed in the wavelength range of 200-700 nm as depicted in Fig. 1.

The Uv−Visible spectrum of the synthesized IONS shows a clear absorption band around 294 nm. The similar pattern of absorption band around 200 to 300 nm for green synthesized iron oxide nanomaterial using plant extract such as *Myristica fragrans* (290 nm) [28], and *Avicenna Marina* (298 nm) [29] supporting the formation of iron oxide species under mild calcination.

Fourier Transform Infrared (FTIR) Analysis

The FTIR spectroscopy was used to analyse the functional groups and chemical bonds formed on the surface of the green synthesized IONS as well as to confirm the role of organic molecules from plant extract in their reduction and stabilization. The FTIR spectrum was monitored in the wavenumber range of 4000−400cm^{-1} as presented in Fig. 2. The broad absorption peak at 3400cm^{-1} is attributed to surface hydroxyl (−OH) groups indicating the presence of residual organic compounds and moisture even after 450°C calcination. Similar observation after thermal treatment have been reported [25.28] in the green synthesis of iron oxide NS, where phytochemicals remain adsorb on the oxide surface and contributed to its stabilization.

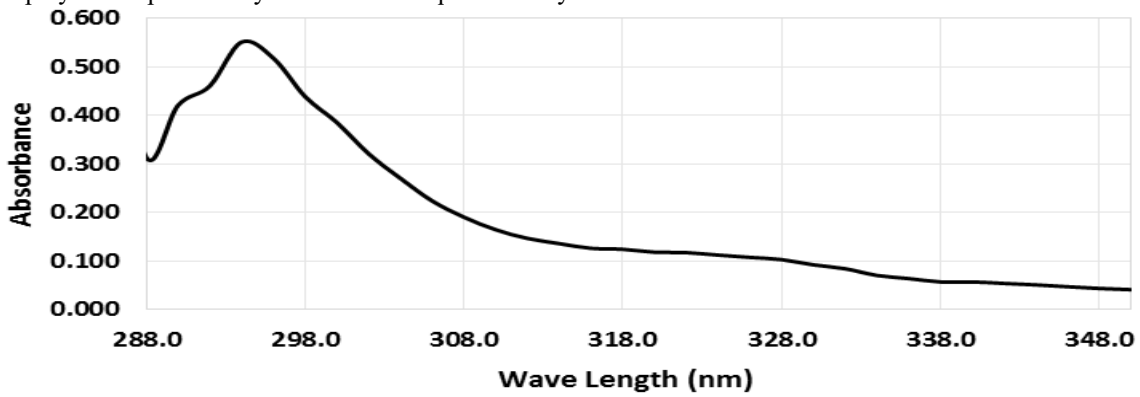

Fig. 1: UV-visible spectra of iron oxide nanostructures (IONS).

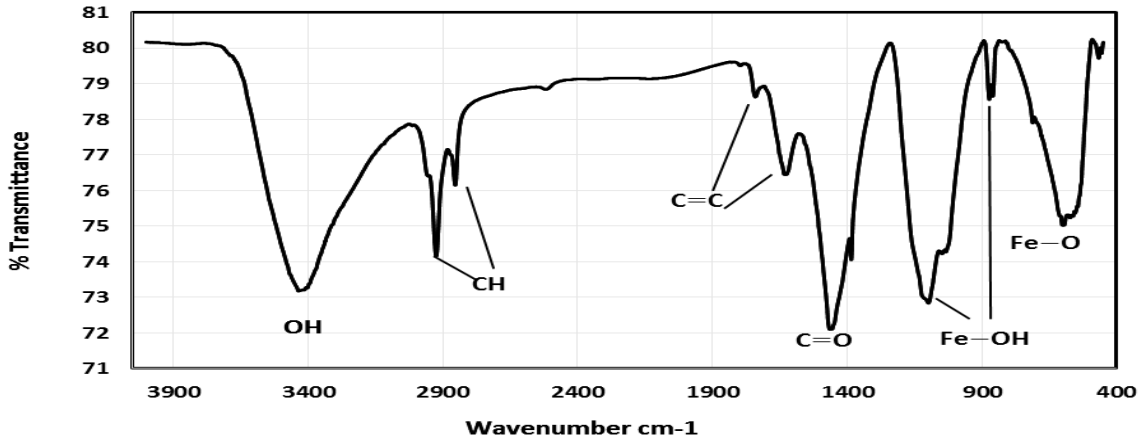

Fig. 2: FT-IR characterization of iron oxide NS.

Moreover the absorption peaks were observed in the range of 2939−2854cm^{-1} are due to C−H stretching vibration of methyl (−CH_3) and methylene (−CH_2) groups, indicating the aliphatic compounds [28]. The weak absorption peak around 1625−1700cm^{-1} may be attributed not only to the C═C stretching vibration of aromatic rings but also to the absorption of water molecules. However, the peak at 845−1150cm^{-1} corresponds to Fe−OH stretching vibration that represents the IONS formation [28].

The most significant high intensity absorption band in the low frequency range 540−575cm^{-1}, with a characteristic peak around 568cm^{-1}, represents the Fe−O stretching vibration, assure the formation of IONS [29-30].

X-Ray Diffraction (XRD) Analysis

XRD analysis reveals that the sustainable IONS are mostly amorphous in nature as confirmed by the weak diffraction peaks. Fig. 3 presented the XRD spectrum that indicates the small diffused peak at 28°, 36° and 43° (2θ) suggesting minor sort range ordering in iron oxide phase. The relatively low and weak peak intensity may be attributed to small crystallite size, low crystallinity and enhanced surfaced capping of phytochemicals from plant extract. Numerous studies reported the same XRD pattern of IONS when plant extract is used as an environmentally friendly reducing agent [25, 31, 32]. On the basis of literature support it is confirmed that the synthesized IONS are identified as amorphous in nature. As there is no sharp Bragg reflection indicates the minimal crystallinity of the IONS [33].

Scanning Electron Microscopy (SEM) Analysis

The surface morphology and structural features of the fabricated IONS were analysed by scanning electron microscopy (SEM) at magnifications of 50x and 100x as presented in Fig. 4.

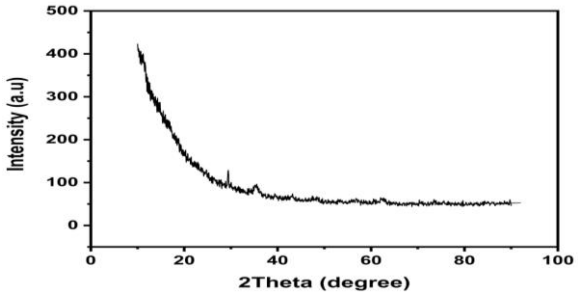

Fig-3: XRD analysis of iron oxide NS.

The SEM micrographs indicating that the synthesized IONS calcined at 450C° large, angular with a high degree of agglomeration. It is observed from the SEM images the NS appears in clusters formed through the aggregation of smaller nanosized particles. The agglomerates have relatively rough surface and noticeable gap between these particles can be observed. Such type of agglomeration may be due to the magnetic interactions of IONS which ultimately increases particle-particle interactions. As well as the presence of phytochemicals residue may contribute in the interparticle interaction as evidenced by the −OH peak observed through FTIR spectrum which supports the cause of agglomeration [36]. Comparable results have been reported by A.Nughwal et al., [34] and S. Salim et al., [31] who worked on the synthesis of iron oxide nanoparticles using the *Argemone mexicana* and *Myristica fragrance* leaf extract. Their studies reported the polydispersed and aggregated morphologies which support the tendency of IONS synthesized through plant extract to form cluster.

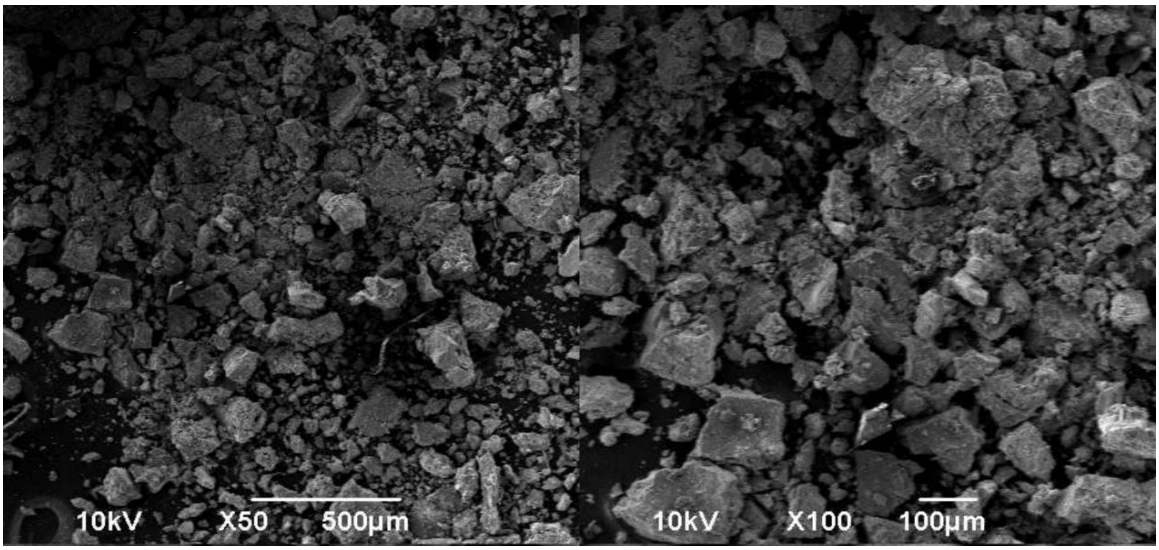

Fig. 4: SEM images of IONS synthesized using *Fagonia indica* plant extract.

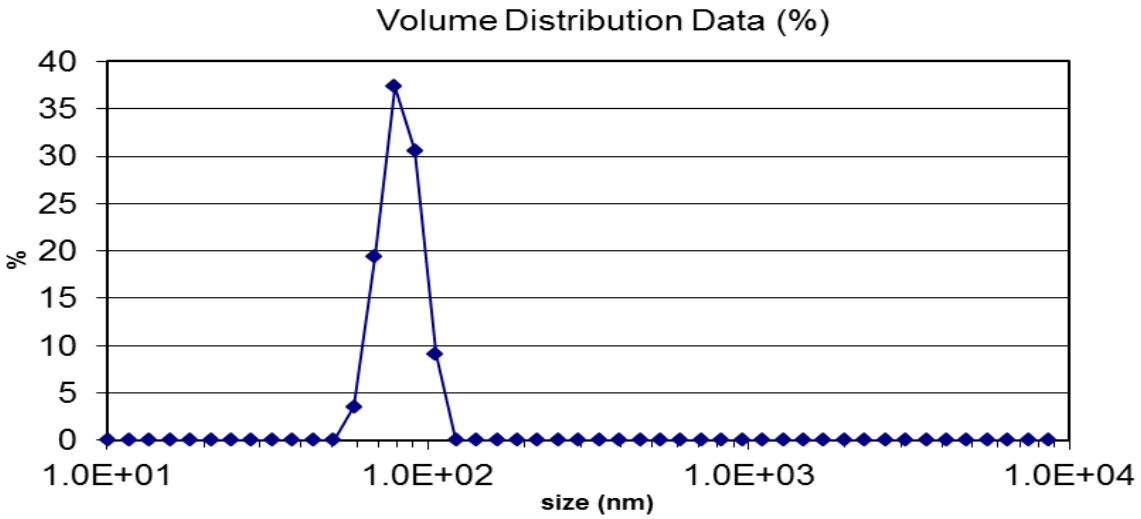

Fig. 5: Volume-weighted particle size distribution of iron oxide NS quantified by DLS.

Particle Size Analysis

Dynamic light scattering (DLS) was used to determine the particle size distribution of the fabricated iron oxide NS via the Malvem DTS software as shown in Fig. 5.

The DLS study revealed a monomodal particle size distribution centered at approximately 78.8 nm with a polydispersity index (PDI) of 0.23, which is inconsistent with the literature reports on plant mediated synthesis of IONP. [35]. The size distribution followed approximately a Gaussian profile with a full width at half maximum (FWHM) of around 30nm, calculated from volume weight distribution representing moderate size dispersion. However the accumulative volume analysis revealed that the majority of particles (86.62%) were distributed in the range of (68−91nm). While minor population of nanostructures (NS) were observed at 59 nm (3.5%) and 105 nm (9.12%) respectively. No particles smaller than 50 nm and larger than 110 nm was detected. DLS measurements reported for IONS synthesis through green routes commonly revealed the hydrodynamic size in the range of (~78−80 nm), which are greater than the primary core nanostructure as a result of nanoparticle dispersion in suspension and interparticle aggregation [36]. Comparable results have been reported by A. S Kachhawaha et al., using *Clitoria ternatia* flower extract

for the synthesis of IONS that showed a hydrodynamic size of around 68.41 nm consistent with moderated colloidal dispersion [37].

Zeta Potential Analysis

The zeta potential of the synthesized IONS was observed as a sharp Gaussian peak in the range of −30 to 0 mV at pH 12 with a highest peak intensity at −16 mV as shown in Fig. 6. It indicating the moderate negative charge surface although no positive charge or secondary charge were detected suggesting moderately charged surface and minimal contamination. Although, the observed value is below the ±30mV threshold value that commonly cited for strong colloidal stability. This indicate the surface of IONS were moderately negative charged promoting dispersion in the medium. However at high pH (12) the surface deprotonation of IONS and formation of $Fe–O^-$ groups on the surface that exhibits some electrostatic repulsion in suspension [38].

The observed zeta potential of −16 mV is consistent with the findings of M. S. H Bhuiyan et al., [39] and A. Nughwal et al., [34] who reported the zeta potential values of −15.1 and −12 mV respectively for IONS using *Carica papaya* and *Argemone maxicana* leaf extracts.

Photocatalytic Degradation

Methylene blue (MB) exhibited noticeable degradation when exposed to sunlight even in the absence of nanocatalyst (IONS), whereas negligible degradation was observed under dark conditions highlighting the essential role of light induced photodegradation processes. The direct photolysis of MB molecules occurs, where photons provide sufficient energy to excite the MB molecules, leading to partial breakdown of their chromophore structure. Comparatively, when IONS induced under dark conditions only a negligible reduction in absorbance was recorded. This behavior is primarily associated with the adsorption of MB molecule onto the surface of the nanostructures rather than true catalytic degradation [40−41]. The comparative results between sunlight only, IONS in dark, and IONS under sunlight is presented in Fig. 7. From the UV-Visible data, it is clearly observed that a pronounced enhancement in MB degradation occurs when iron IONS are exposed to sunlight indicating a strong synergistic interaction between solar irradiation and photo catalyst. Upon sunlight exposure the IONS absorb photons and generate electron-hole pairs ($\bar{e}$—h^+). The photgenerated holes (h^+) reacts with surface hydroxyl ions or water molecules to produced highly stable hydroxyl radical ($^\bullet OH$), while the excited electrons ($\bar{e}$) interact with dissolved Oxygen O_2 to form superoxide radicals ($^\bullet O_2^-$). These reactive oxygen species play a crucial role in the oxidative degradation of MB by attacking the aromatic ring and conjugated chromophore system, ultimately leading to mineralization into smaller, less harmful molecules such a CO_2, H_2O and inorganic ions [16, 42].

The significantly higher degradation efficiency observed in the presence of both sunlight and IONS confirms the photolytic nature of the process rather than simple adsorption or photolysis. This enhanced activity demonstrate the ability of IONS to effectively utilize solar energy to accelerate dye degradation thereby reducing reaction time and improving treatment efficiency [16].

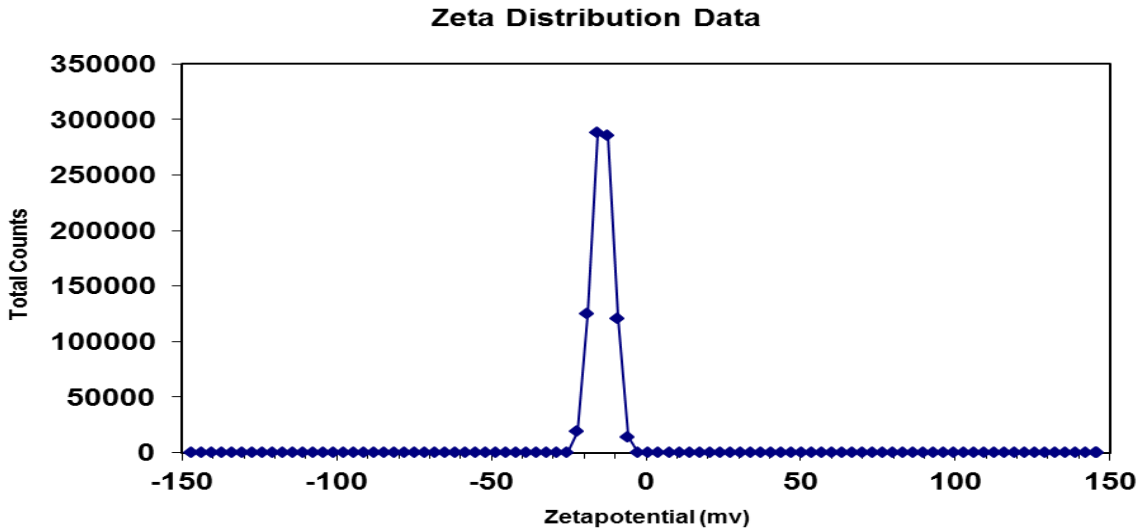

Fig. 6: Zeta potential intensity distribution of iron oxide NS analysed by DLS.

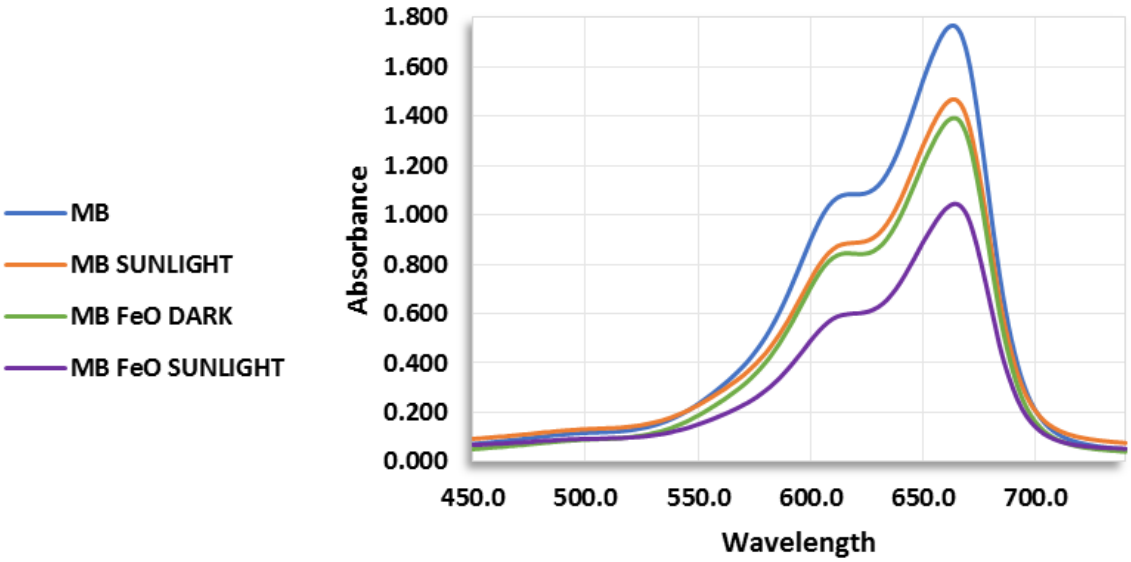

Fig. 7: Degradation of MB under dark and sunlight conditions with and without NS.

Effect of pH of Solution on Dye Degradation

UV-Visible spectroscopic analysis (Fig. 8) revealed that the photocatalytic degradation of 10 ppm solution of MB by plant mediated IONS is strongly pH dependent. The efficiency of degradation was increasing progressively from acidic to alkaline conditions. Minimum degradation was observed at pH 3, which increased to approximately 33% at pH 6, ~ 45% at pH 9 and reached a maximum of approximately 52% at pH 12. At high pH the surface of IONS becomes negative due to deprotonation. This promote the stronger electrostatic interaction between cationic MB dye molecule and negatively charged surface of catalyst adsorbent, resulting in improved adsorption efficiency [43]. Moreover alkaline conditions provides a higher concentration ions of hydroxyl ions (OH^-), which readily react photogenerated holes (h^+) on the nanomaterial surface to generate highly reactive hydroxyl radicals ($^\bullet OH$), the primary oxidative species responsible for dye degradation. Increased availability of OH^- ions also suppresses electron─hole recombination, prolonging charge carrier lifetimes and enhancing reactive oxygen species [16]. Similar, pH dependent behaviour has been widely reported for several other metals photocatalyst confirming that alkaline environments favour enhanced photocatalytic degradation of cationic dyes such as MB through improved adsorption, radical generation and charge transfer processes [44].

Effect of Initial Dye Concentration

The photocatalytic degradation of MB using 20mg of IONS was analysed at initial dye concentration of 4, 8, 12 and 16 ppm under the optimized pH of 12. UV– Visible studies (Fig. 9) showed the concentration depended decline in MB dye degradation, with removal efficiencies of 58.454% for 4ppm, 55.51% for 8ppm, 48.50% for 12ppm and 46.40% for 16ppm respectively. The reduction in degradation efficiency at higher concentration is possibly due to the saturation of active sites on the IONS surface and diminution of light penetration, which together limit the creation of reactive photogenerated reactive species essential for degradation of dyes [16]. Among the studied concentrations, 8ppm giving the most effective performance achieving 55.51% degradation capacity of 8µg dye degraded per mg of IONS catalyst. The photocatalytic degradation efficacy depends on the initial dye concentration, with increased concentration causes the light screening effect that reduce photon penetration and supresses electron hole pair generation [45]. Relatively similar observation has been reported by S.S. Priyadharshini et al., for the photocatalytic degradation of ZnO nanocatalyst under Uv irradiation. It showed progressive decrease in degradation efficiency as MB dye concentration from 5ppm to 20pppm increased, since higher dye concentration diminishes the reactive species specific for degradation [46].

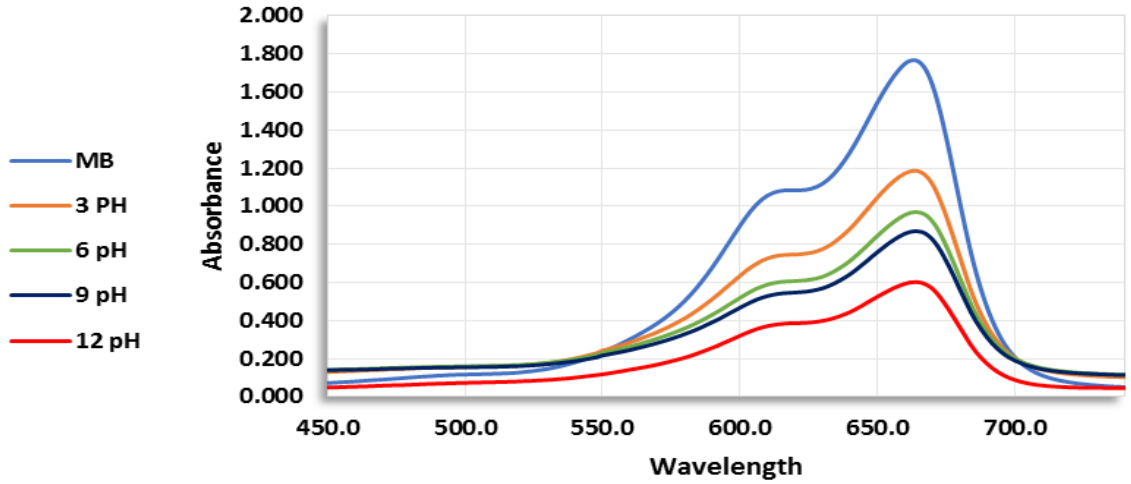

Fig. 8: Effect of pH on MB degradation.

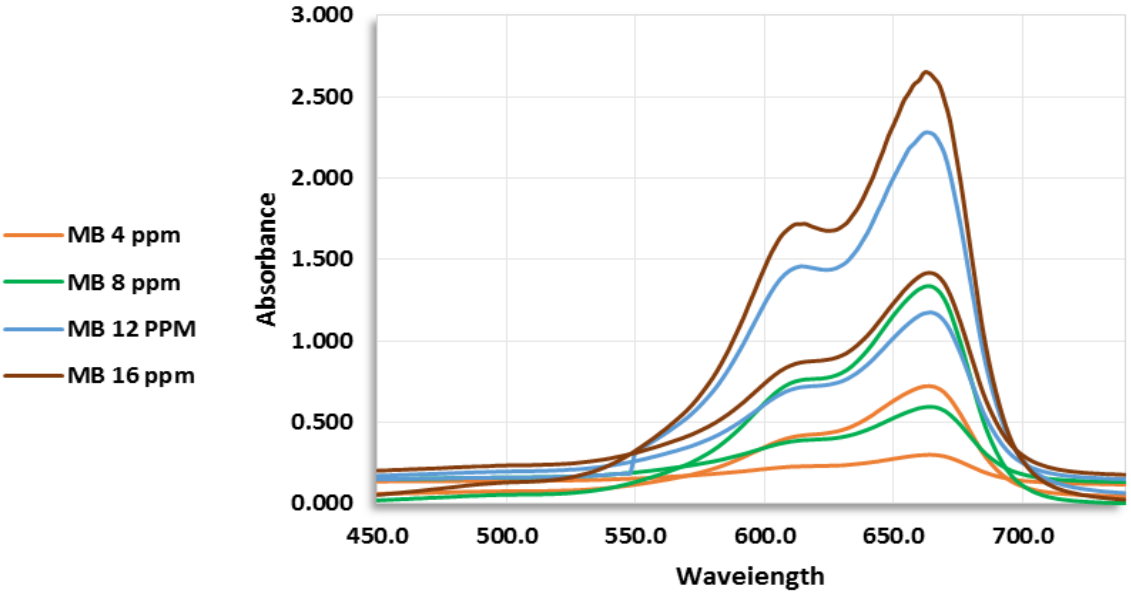

Fig. 9: Effect of initial MB concentration on degradation.

Effect of Iron Oxide Dosage on Methylene Blue Degradation

The effect of IONS dosage on the photocatalytic degradation of MB (10ppm) was systematically investigated at the optimized pH of 12 under visible light irradiation. 20, 30, 40 and 50 mg of IONS were evaluated to determine the optimal loading for maximum degradation efficiency. It is signified that 80.0% MB dye degraded progressively with increased IONS amount from 20 to 40mg as shown in Fig. 10. This enhancement can be attributed to the increased availability of active sites on the NS surface, which facilitate hydroxyl radical ($^{\bullet}OH^{-}$) and superoxide anions radical ($O_2^{\bullet-}$) responsible of oxidative degradation. Only a marginal improvement in degradation efficiency was observed after increasing the amount of IONS from 40mg (80.0%) to 50mg (82.4%). Therefore 40 mg was selected as the optimum dosage for further optimization process. Comparable trends have been reported widely for metal oxide photocatalyst, where excessive catalyst aunt cause agglomeration and light scattering, eventually restraining photon penetration and reducing photocatalytic efficiency [47].

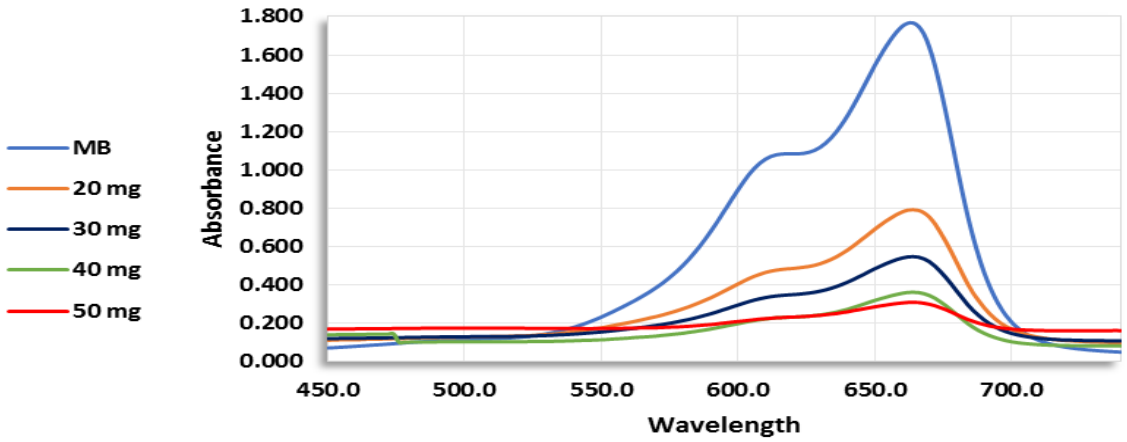

Fig. 10: Effect of Iron Oxide dosage on MB degradation.

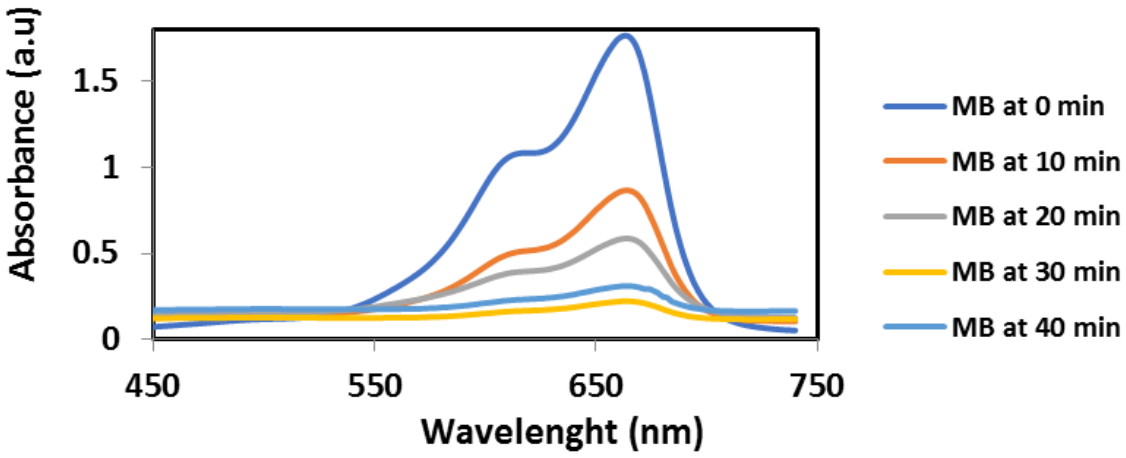

Fig. 11: Degradation of MB with respect to time.

Degradation of MB with Respect to Time

The effect of irradiation time on the photocatalytic degradation of MB (10ppm) using 40mg of IONS was monitored by UV Visible spectroscopy at the characteristics absorption maximum of ~664 nm (Fig. 11). The degradation profile exhibited two distinct phases: an initial rapid adsorption dominated stage (0−20min), during which a large portion of MB approximately 67% was removed due to electrostatic interaction and surface adsorption onto the high surface area of IONS followed by a slower controlled phase (20−40min), where photocatalytic reaction govern promote dye decomposition. Under optimized condition ~87.5% of MB degraded within 40 min. However, no significant shift in the wavelength of maximum absorption was observed confirming the dye degradation rather than transformation into intermediate species. Similar studies reported the multistage degradation of MB dye by using Fe_2O_3/TiO_2 and Clay@Fe_3O_4 as a nanocatalyst [48−49].

Pseudo First Order Kinetics of Dye Degradation

The kinetic of photodegradation under UV−Visible light was monitored at different time intervals. The degradation kinetics was evaluated using a pseudo first order reaction by calculating $-\ln(A_t/A_o)$, and the corresponding values are presented in Fig.12.

The rate constant (eq: 2) for this reaction was calculated after plotting $-\ln A_t/A_o$ vs irradiation time. The rate constant of 0.0519 min^{-1} lies within the range and support the catalytic efficiency of *Fagonia indica* mediated IONS for degradation of dye.

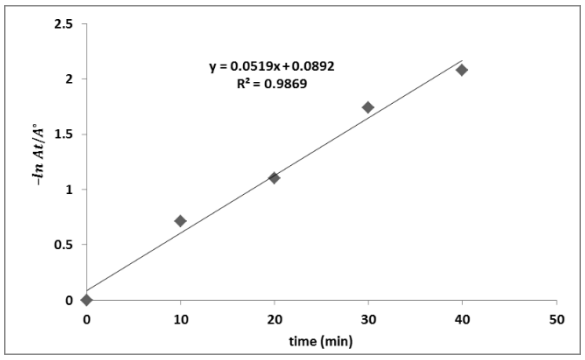

Fig. 12: Pseudo-first-order kinetics of MB degradation under Uv-Visible irradiation.

The half−life (eq:3) which is characteristics of first order reaction kinetics was calculated to be approximately 13.3min and about 87.5% dye degradation was achieved within 40 min. It strongly supports the pseudo first order kinetics behaviour of, indication that the efficiency of dye degradation is directly related to dye concentration. Photocatalysis is primarily a surface driven process, and amorphous hydroxide with abundant surface ($-OH^{-1}$) groups can efficiently generate reactive oxygen species under light driven irradiation. Several studies on green synthesized IONS have been reported higher degradation efficiencies (≈70−95%) for MB degradation. The IONS observed efficiency of 87.5% in this study is analogous to the range of reported studies indicating IONS exhibit competitive photodegradation efficiency regardless of relatively large particle size [50−51].

$$-\ln\frac{A_t}{A_\circ} = kt \qquad \text{(eq: 2)}$$

$$t_{1/2} = \frac{0.693}{k} \qquad \text{(eq :3)}$$

Conclusion

The iron oxide nanostructures (IONS), prepared by means of the *Fagonia indica* plant extract, revealed excellent activity for photocatalytic degradation of organic dyes in sunlight. The green, low cost and simple route followed for the synthesis and the resulting IONS were agglomerated and 78.8 nm in size with a zeta potential of −16mV indicating moderate colloidal stability supported by the phytochemicals from plat extract. XRD analysis revealed the amorphous nature of IONS. SEM analysis showed relatively large agglomerated particles due to electrostatic interaction and magnetic nature of iron oxide. The IONS showed excellent catalytic efficacy for the MB dye using 40mg of optimized amount the dye degraded 87.5% within time period of 40mins. The reaction kinetic was monitored and the half-life and rate constant of 13.3min and 0.056 min^{-1} were calculated respectively. The reaction kinetics followed pseudo first order kinetics which suggests that the rate of reaction mainly depend on the concentration of MB dye. This study uses the *Fagonia indica* plant first time for the synthesis of IONS. It also provide cost effective strategy for waste water treatment and highlight the potential of medical plant assisted synthesis for environmental remediation and application by replacing toxic organic reducing agents.

Acknowledgment

The author thanks to Dr. M. A. Kazi Institute of Chemistry for completion of this work

References

1. P. K. Singh, U. Kumar, I. Kumar, A. Dwivedi, P. Singh, S. Mishra, C. S. Seth and R. K. Sharma, Critical review on toxic contaminants in surface water ecosystem: sources, monitoring, and its impact on human health, *Environ. Sci. Pollut. Res.*, **31**, 56428–56462 (2024).
2. K. Waseem, A. S. Akhtar and A. Nawaz, Water quality assessment and trends in twin cities of Pakistan: a review, *Discover Water*, **4**, 125 (2024).
3. M. F. Tariq, F. Javed, L. Rizzo, M. W. Tahir and A. Ikhlaq, Textile wastewater treatment by heterogeneous catalytic ozonation using microcellulose loaded ZIF-67 catalyst, *J. Environ. Manage.*, **380**, 125031 (2025).
4. H. H. Iqbal, A. Siddique and A. Qadir, Human health and ecology at risk: a case study of metal pollution in Lahore, Pakistan, *Environ. Sci. Eur.*, **36**, 9 (2024).
5. F. Majeed, A. Razzaq, S. Rehmat, I. Azhar, A. Mohyuddin and N. Rizvi, Enhanced dye sequestration with natural polysaccharides-based hydrogels: a review, *Carbohydr. Polym.*, **330**, 121820 (2024).
6. S. Sehar, T. Rasool, H. M. Syed, M. A. Mir, I. Naz, A. Rehman, M. S. Shah, M. S. Akhter, Q. Mahmood and A. Younis, Recent advances in biodecolorization and biodegradation of environmental threatening textile finishing dyes, *3 Biotech*, **12**, 186 (2022).
7. H. Patel, V. K. Yadav, K. K. Yadav, N. Choudhary, H. Kalasariya, M. M. Alam, A. Gacem, M. Amanullah, H. A. Ibrahium, J.-W. Park, S. Park and B.-H. Jeon, A recent and systemic approach towards microbial

biodegradation of dyes from textile industries, *Water*, **14**, 3163 (2022).
8. T. Robinson, G. McMullan, R. Marchant and P. Nigam, Remediation of dyes in textile effluent: a critical review on current treatment technologies with a proposed alternative, *Bioresour. Technol.*, **77**, 247–255 (2001).
9. E. Forgacs, T. Cserháti and G. Oros, Removal of synthetic dyes from wastewaters: a review, *Environ. Int.*, **30**, 953–971 (2004).
10. V. Katheresan, J. Kansedo and S. Y. Lau, Efficiency of various recent wastewater dye removal methods: a review, *J. Environ. Chem. Eng.*, **6**, 4676–4697 (2018).
11. M. R. Hoffmann, S. T. Martin, W. Choi and D. W. Bahnemann, Environmental applications of semiconductor photocatalysis, *Chem. Rev.*, **95**, 69–96 (1995).
12. M. N. Chong, B. Jin, C. W. K. Chow and C. Saint, Recent developments in photocatalytic water treatment technology: a review, *Water Res.*, **44**, 2997–3027 (2010).
13. N. Zhang, Y. Zhang and Y.-J. Xu, Recent progress on graphene-based photocatalysts: current status and future perspectives, *Nanoscale*, **4**, 5792–5813 (2012).
14. I. Khan, K. Saeed and I. Khan, Nanoparticles: properties, applications and toxicities, *Arab. J. Chem.*, **12**, 908–931 (2019).
15. P. R. S. Baabu, H. K. Kumar, M. B. Gumpu, J. B. K. Babu, A. J. Kulandaisamy and J. B. B. Rayappan, Iron oxide nanoparticles: a review on the province of its compounds, properties and biological applications, *Materials*, **16**, 59 (2022).
16. D. Khadka et al., Evaluating the photocatalytic activity of green synthesized iron oxide nanoparticles, *Catalysts*, **14**, 751 (2024).
17. P. Singh et al., Systematic review on applicability of magnetic iron oxides–integrated photocatalysts, *Mater. Today Chem.*, **14**, 100186 (2019).
18. P. R. Chowdhury et al., Photocatalysis: TiO_2, ZnO, and iron oxides, *Nanoremediation*, —, 101–126 (2023).
19. M. Afkari et al., Effects of iron oxide contents on photocatalytic performance of g-C3N4 nanocomposites, *Sci. Rep.*, **13**, 6203 (2023).
20. S. Ahmed, S. Inayat and I. Javed, Synthesis methods and characterization of iron oxide nanoparticles, *Synth. Sinter.*, **5**, 109–128 (2025).
21. M. S. Qureshi et al., Comparative analysis of Fagonia indica extracts and green nanoparticles, *Sci. Rep.*, **15**, 37177 (2025).
22. R. Hussain et al., Zinc oxide nanoparticles using Fagonia blend microbial arrest, *Appl. Biochem. Biotechnol.*, **195**, 264–282 (2023).
23. H. R. El-Seedi et al., Updated review of metal nanoparticles fabricated by green chemistry, *Bioengineering*, **11**, 1095 (2024).
24. S. Shivani et al., Iron oxide nanoparticles: synthesis and degradation of methyl red, *Appl. Phys. A*, **131**, 649 (2025).
25. S. K. Begum et al., Green synthesis of Fe_3O_4 and Fe_2O_3 nanoparticles, *Sci. Rep.*, **15**, 36465 (2025).
26. A. Q. Malik et al., Review on green synthesis of nanoparticles, *Environ. Sci. Pollut. Res.*, **30**, 69796–69823 (2023).
27. M. B. Goudjil et al., Photocatalytic degradation of methylene blue using α-Fe_2O_3, *Desalin. Water Treat.*, **317**, 100079 (2024).
28. S. Salim et al., Green synthesis of iron oxide nanoparticles using Myristica fragrans, *Microbe*, **8**, 100481 (2025).
29. P. Karpagavinayagam and C. Vedhi, Green synthesis using Avicennia marina, *Vacuum*, **160**, 286–292 (2019).
30. F. K. da Silva Naves et al., Catalytic potential of green iron nanoparticles, *Green Chem. Technol.*, **2**, 10018 (2025).
31. M. A. J. Kouhbanani et al., Green synthesis using Teucrium polium, *Adv. Nat. Sci. Nanotechnol.*, **10**, 015007 (2019).
32. F. K. da S. Naves et al., Eucalyptus grandis iron nanoparticles, *Rev. Ambiente Água*, **19**, e2978 (2024).
33. M. A. Khan et al., Citrus limetta-derived Fe_2O_3 nanoparticles, *Sci. Rep.*, **15**, 33107 (2025).
34. A. Nughwal et al., Argemone mexicana iron nanoparticles, *RSC Adv.*, **15**, 10287–10297 (2025).
35. K. S. John et al., Ocimum gratissimum nanofertilizer application, *Discover Appl. Sci.*, **6**, 542 (2024).
36. H. S. Devi et al., Iron oxide nanoparticles antifungal activity, *Green Process. Synth.*, **8**, 38–45 (2019).
37. A. S. Kachhawaha et al., Clitoria ternatea iron nanoparticles antibacterial evaluation, *Biomed. Pharmacol. J.*, **18**, (2025).
38. T. T. Win et al., Fe_3O_4 nanoparticles using Chlorella extract, *Sci. Rep.*, **11**, 21996 (2021).
39. M. S. H. Bhuiyan et al., Carica papaya iron nanoparticles for dye degradation, *Heliyon*, **6**, e04603 (2020).
40. S. Abdelghany et al., Iron oxide/silver nanoparticles biological evaluation, *Sci. Rep.*, **15**, 29593 (2025).
41. D. M. Osorio-Aguilar et al., Methlyene blue adsorption review, *Catalysts*, **13**, 1480 (2023).

42. R. Vilés-Monreal et al., Fe_3O_4–Fe_2O_3 photocatalysis on mordenite, *SN Appl. Sci.*, **5**, 389 (2023).
43. M. Khalifa et al., Pyridine-thiazole adsorbent for dye removal, *Sci. Rep.*, **15**, 39016 (2025).
44. A. A. Melegy et al., Fe_3O_4/ZnO/$ZnFe_2O_4$ photocatalysts, *Sci. Rep.*, **15**, 26333 (2025).
45. S. Nehhal et al., ZnO photocatalysis under LED light, *Reactions*, **6**, 64 (2025).
46. S. S. Priyadharshini et al., ZnO nanocrystals for dye degradation, *Crystals*, **12**, 22 (2022).
47. A. Melegy et al., Superparamagnetic Fe_3O_4/ZnO composites, *Sci. Rep.*, **15**, 40393 (2025).
48. L. Liu et al., Fe_2O_3/TiO_2 photocatalytic composites, *Materials*, **17**, 4546 (2024).
49. A. Aboussabek et al., Clay@Fe_3O_4 for methylene blue removal, *Case Stud. Chem. Environ. Eng.*, **9**, 100580 (2023).
50. V. Jadhav et al., Ag-doped iron oxide nanostructures, *Discover Nano*, **20**, 66 (2025).
51. D. Purushotham et al., ZnO nanoparticles for methylene blue degradation, *Int. J. Mol. Sci.*, **26**, 4739 (2025).